Electronic Supplementary Material (ESI) for Soft Matter.

Adsorption Parameters and Phase Behaviour of Non-Ionic Surfactants at Liquid Interfaces

(electronic supplementary information)

Radomir Iliev Slavchov[#,*], Ivan Boyanov Ivanov[‡]

 # Department of Chemical Engineering and Biotechnology, Cambridge University, UK, CB3 0AS Cambridge

‡ Laboratory of Chemical Physics and Engineering, Faculty of Chemistry and Pharmacy, Sofia University

Contents:

S1. Adsorption models: summary of the formulae

Table S1. Equations of state and surface activity coefficients (adsorption isotherms) of various adsorption models.

Continual models		
model	π^S/k_BT **(EoS)**	$\ln\gamma^S$ **(adsorption isotherm** $K_aC = \gamma^S\Gamma$**)**
Henry	Γ	0
virial	$\Gamma + B_2\Gamma^2 + O(\Gamma^3)$, $K_aC - B_2(K_aC)^2 + O(C^3)$	$2B_2\Gamma + O(\Gamma^2)$
HFL	$\frac{\Gamma}{(1-\alpha\Gamma)^2}$	$-\ln(1-\alpha\Gamma) + \frac{\alpha\Gamma(3-2\alpha\Gamma)}{(1-\alpha\Gamma)^2}$
SIAL	$\frac{\Gamma}{(1-\alpha\Gamma)^2} - \beta\alpha\Gamma^2$	$-\ln(1-\alpha\Gamma) + \frac{\alpha\Gamma(3-2\alpha\Gamma)}{(1-\alpha\Gamma)^2} - 2\beta\alpha\Gamma$
SD	$\frac{R_\beta - 1}{2\alpha\beta(1-\alpha\Gamma)}$, $R_\beta = \sqrt{1+4\beta\frac{\alpha\Gamma}{1-\alpha\Gamma}}$	$-\ln(1-\alpha\Gamma) + \left(2+\frac{1}{\beta}\right)\ln\frac{2}{1+R_\beta}$ $+\frac{\alpha\Gamma(4-3\alpha\Gamma)}{(1-\alpha\Gamma)^2}\frac{2}{1+R_\beta}$
Volmer	$\frac{\Gamma}{1-\alpha_V\Gamma}$	$-\ln(1-\alpha_V\Gamma) + \frac{\alpha_V\Gamma}{1-\alpha_V\Gamma}$
vdW	$\frac{\Gamma}{1-\alpha_V\Gamma} - \beta_V\alpha_V\Gamma^2$	$-\ln(1-\alpha_V\Gamma) + \frac{\alpha_V\Gamma}{1-\alpha_V\Gamma} - 2\beta_V\alpha_V\Gamma$
Langmuir	$-\frac{\ln(1-\alpha_L\Gamma)}{\alpha_L}$	$-\ln(1-\alpha_L\Gamma)$
Frumkin	$-\frac{\ln(1-\alpha_L\Gamma)}{\alpha_L} - \beta_L\alpha_L\Gamma^2$	$-\ln(1-\alpha_L\Gamma) - 2\beta_L\alpha_L\Gamma$

S2. The adsorption constant K_a

In this section, the adsorption constant K_a will be related to the surfactant structure and the parameters of the media (temperature, bulk compositions etc.) through a model proposed by Ivanov et al. [49,7,8] for the interaction free energy $\Delta\mu(z)$ of a surfactant molecule with the interface. The main contributions to $\Delta\mu(z)$ which were taken into account in this model are summarized below.

a) Contribution of the hydrophobic solvation of surfactant's linear hydrocarbon chain. The adsorption of a surfactant molecule from the water phase to the interface is due mostly to the hydrophobic effect [68,65], i.e. to the change of the free energy of the hydrophobic tail upon its transfer from the hydrophobic phase to the water phase. Let this transfer energy per single $–CH_2–$ group be $\Delta\mu_{CH_2}$ ($\Delta\mu_{CH_2} > 0$). We will denote the length of a $–CH_2–$ group along the hydrophobic chain by l_{CH_2} (l_{CH_2} =1.26 Å [65,68]) and the number of the carbon atoms in the hydrocarbon chain by n (therefore, the total chain length, including the $–CH_3$ end, is close to nl_{CH_2}). We will use the symbol z for the distance between the interface and the "hydrophilic-lyophilic centre" of the surfactant, which is the point where the hydrophilic head and the hydrophobic chain are connected [78,68]. For simplicity, we assume that the surfactant molecule remains perpendicular to the interface during the adsorption process. Then, if $z < nl_{CH_2}$, a portion of the surfactant hydrocarbon chain of length $nl_{CH_2} – z$ will be immersed into the hydrophobic phase. This corresponds to a free energy change $–(n – z/l_{CH_2})\Delta\mu_{CH_2}$ upon transfer of a molecule from the bulk to a distance z from the interface [49]. The result is, however, not entirely correct, since the end $–CH_3$ group has different area and adsorption energy from a $–CH_2–$ group. We account for this by introducing in the energy $–(n – z/l_{CH_2})\Delta\mu_{CH_2}$ a correction term $\Delta\mu_{CH_3} – \Delta\mu_{CH_2}$ equal to the extra adsorption energy of the methyl group with respect to a $–CH_2–$. This yields [49]:

$$\Delta\mu_h(z) = \begin{cases} -\Delta\mu_{CH_3} - \left(n - 1 - z/l_{CH_2}\right)\Delta\mu_{CH_2}, & z < nl_{CH_2}; \\ 0, & z > nl_{CH_2}. \end{cases} \tag{31}$$

b) Contribution of the disappearing interfacial area. Upon adsorption, the hydrocarbon chain penetrates the interface, and a portion of the interface is replaced by the chain [49,7,6]. If the cross-sectional area of the chain is $\alpha_\perp$, then the contribution of this replacement to the adsorption energy is equal to $-\alpha_\perp\sigma_0$, where σ_0 is the interfacial tension of the pure interface. Assuming that this energy is gained at the moment of contact between the hydrocarbon chain and the interface (at $z = nl_{CH_2}$), we can write the corresponding potential profile $\Delta\mu_\sigma$ as [49]:

$$\Delta\mu_{\sigma}(z)=\begin{cases}-\alpha_{\perp}\sigma_0, & z<nl_{CH_2};\\ 0, & z>nl_{CH_2}.\end{cases} \tag{32}$$

The significance of this term for the dependence of the adsorption constant K_a at W|O interface on the nature of the oil phase is discussed in Ref. [7]. The linear dependence of $\ln K_a$ on σ_0 was confirmed there by using data of Rehfeld [102] for the adsorption isotherms of the ionic surfactant sodium dodecylsulfate on various W|O interfaces which allow determination of K_a as a function of σ_0 only. The term $\alpha_{\perp}\sigma_0$ has a large contribution to the enthalpy of adsorption, and therefore, determines to a large extent the temperature dependence of K_a (*figure 8* in Ref. [8]).

c) Contribution of rotation. In order to estimate the contribution of the rotational degrees of freedom of the adsorbed molecule to the adsorption constant K_a, let us first calculate the partition functions for the initial (in the bulk) and the final (at the surface) states. For simplicity we assume that the molecule rotates as a solid stick of inertial moment I. The Hamiltonian of a freely rotating stick in spherical (r,ϑ,φ) coordinates is [59]:

$$H=\left(p_{\vartheta}^2+p_{\varphi}^2/\sin^2\vartheta\right)/2I\,. \tag{33}$$

Here p_{ϑ} and p_{φ} are the respective momenta of the stick. This Hamiltonian corresponds to bulk partition function (*Eq. 8-27* of Hill [59]):

$$q_{rot}^{B}=\frac{1}{h^2}\int_{-\infty}^{\infty}\int_{-\infty}^{\infty}\int_{0}^{\pi}\int_{0}^{2\pi}e^{-H/k_BT}\,d\varphi d\vartheta dp_{\varphi}dp_{\vartheta}=8\pi^2k_BTI/h^2, \tag{34}$$

where h is Planck constant. For a surfactant molecule at the interface, we assume that this rotation is again free but restricted to the semi-space $z < 0$. This yields for the surface partition function q_{rot}^{S}:

$$q_{rot}^{S}=\frac{1}{h^2}\int_{-\infty}^{\infty}\int_{-\infty}^{\infty}\int_{0}^{\pi/2}\int_{0}^{2\pi}e^{-H/k_BT}\,d\varphi d\vartheta dp_{\varphi}dp_{\vartheta}=4\pi^2k_BTI/h^2\,. \tag{35}$$

It follows from Eqs. (34)&(35) that when the molecule is far from the interface, the free energy of rotation is:

$$f_{rot}(z>nl_{CH_2})=-k_BT\ln\left(4\pi^2k_BTI/h^2\right), \tag{36}$$

and when it is precisely at $z = 0$,

$$f_{rot}(z=0)=-k_BT\ln\left(2\pi^2k_BTI/h^2\right). \tag{37}$$

Upon transfer to $z = 0$, the surfactant molecule is losing total rotational free energy $\Delta f_{rot}(z = 0) = f_{rot}(z = 0) - f_{rot}(z > nl_{CH_2}) = k_BT\ln 2$. The local shape of $f_{rot}(z)$ in the interval $nl_{CH_2} > z > 0$ is relatively unimportant for the final result for K_a, except for too short-chained surfactants. Therefore, for the sake

of simplicity, similarly to Eqs. (31)&(32), we approximate Δf_{rot} with a simple step-function:

$$\Delta\mu_{\text{rot}} = \begin{cases} k_{\text{B}}T\ln 2, & z < nl_{\text{CH}_2}; \\ 0, & z > nl_{\text{CH}_2}. \end{cases} \tag{38}$$

The difference between Δf_{rot} and $\Delta\mu_{\text{rot}}$ is disregarded.

d) Contribution of the hydration of the head group. We assume that the head group cannot be dehydrated and desorbed into the hydrophobic phase. This is equivalent to a hard-wall potential: $\Delta\mu(z) = \infty$ at $z < 0$.

e) Other contributions. There are other factors, which also contribute to the adsorption energy: (**i**) The interaction between the hydrophilic head group and the interface at $z > 0$; (**ii**) Appearance of an induced dipole moment involving the –CH_2– group adjacent to the polar hydrophilic head, which acts oppositely to the hydrophobic effect and leads to immersion of the methylene group into the water phase (cf. *chap. 3* of Ref. [68]). (**iii**) Changes in the internal degrees of freedom (vibration and internal rotation) of the molecule upon adsorption. The latter effect is involved to a certain extent in the transfer energy $n\Delta\mu_{\text{CH}_2}$ of the surfactant chain from the hydrophobic phase to the water and since we are using experimental values for $\Delta\mu_{\text{CH}_2}$, it is probably accounted for implicitly in our model. **(iv)** The approximated nature of our equations for the contributions **a-d**) can also affect the final result for the adsorption energy. Since the effects (**i-iv**) are still not well-understood, we account for them by adding to the total adsorption energy of the surfactant an empirical constant $\Delta\mu_{\text{head}}$ encompassing all of them – its contribution will be analysed post-factum, by comparing theoretical results with the experimental data (Sec. 3.1).

Combining Eqs. (31),(32)&(38) with the contributions **d)** and **e)**, one obtains for $\Delta\mu(z)$:

$$\Delta\mu(z) = \begin{cases} \infty, & z < 0; \\ -E_{\text{a}} + k_{\text{B}}T\ln 2 + \Delta\mu_{\text{CH}_2} z / l_{\text{CH}_2}, & z < nl_{\text{CH}_2}; \\ 0, & z > nl_{\text{CH}_2}. \end{cases} \tag{39}$$

Here the *adsorption free energy* E_{a} stands for the expression:

$$E_{\text{a}} = (n-1)\Delta\mu_{\text{CH}_2} + \Delta\mu_{\text{CH}_3} + \alpha_{\perp}\sigma_0 + \Delta\mu_{\text{head}}. \tag{40}$$

Eq. (39) is illustrated in Fig. S1.

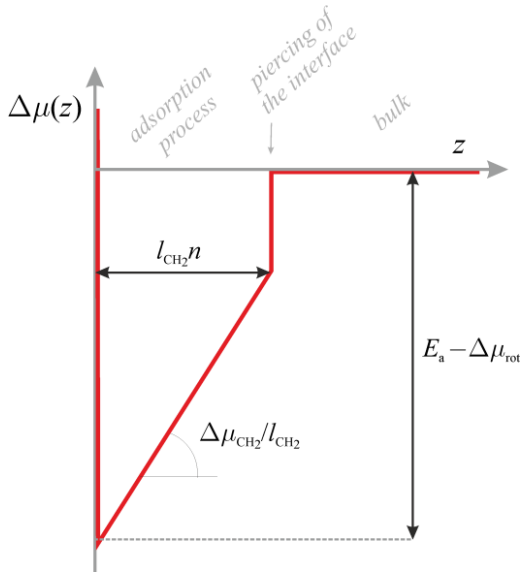

Fig. S1. Interaction potential $\Delta\mu(z)$ between a surfactant molecule and the interface as a function of the distance z between the surfactant hydrophilic-lyophilic centre and the interface, cf. Eq. (39). According to the model, at distance $z > nl_{CH_2}$, there is no significant interaction. At $z = nl_{CH_2}$, energy is gained due to the disappearance of clean water surface of area $\alpha_\perp$, and the transfer energy of the $-CH_3$ group, cf. Eq. (32). At shorter distances, there is a linear dependence of $\Delta\mu$ on z related to the energy of transfer $n\Delta\mu_{CH_2}$ of the hydrocarbon chain from water to the hydrophobic phase, see Eq. (31).

Let us now consider an ideal surfactant solution of concentration C. The local chemical potential $\mu(z)$ of a molecule at a distance z from the interface is:

$$\mu(z) = \mu_0^{\mathrm{B}} + k_{\mathrm{B}}T \ln C^{\mathrm{S}}(z) + \Delta\mu(z)\,. \tag{41}$$

Here, $C^{\mathrm{S}}(z)$ is the local concentration of surfactant near the surface. From the condition $\mu(z) = \mu^{\mathrm{B}} = \mu_0^{\mathrm{B}} + k_{\mathrm{B}}T\ln C$ for chemical equilibrium, the Boltzmann distribution of the surfactant molecules follows:

$$C^{\mathrm{S}}(z) = C\exp(-\Delta\mu(z)/k_{\mathrm{B}}T)\,. \tag{42}$$

Inserting this distribution into Gibbs definition of adsorption, one obtains Henry's adsorption isotherm:

$$\Gamma = \int_0^\infty \left(C^{\mathrm{S}}(z) - C\right)\mathrm{d}z \equiv K_{\mathrm{a}}C\,, \tag{43}$$

where the adsorption constant of the surfactant K_{a} is defined as:

$$K_{\mathrm{a}} = \int_0^\infty \left[\exp(-\Delta\mu(z)/k_{\mathrm{B}}T) - 1\right]\mathrm{d}z\,. \tag{44}$$

It follows from this derivation that Henry's isotherm (43) is valid if the surface-molecule interaction potential $\Delta\mu(z)$ is independent on $C(z)$, which is the case of dilute adsorption layer. Inserting the

expression (39) for $\Delta\mu(z)$ into the definition (44) of K_a and performing the integration, one obtains:

$$K_a = \int_0^{nl_{CH_2}} \left(\frac{1}{2} e^{\frac{E_a - \Delta\mu_{CH_2} z/l_{CH_2}}{k_B T}} - 1 \right) dz = \frac{l_{CH_2} k_B T}{2\Delta\mu_{CH_2}} e^{E_a/k_B T} \left(1 - e^{-n\Delta\mu_{CH_2}/k_B T}\right) - nl_{CH_2} \approx \delta_a e^{E_a/k_B T}, \quad (45)$$

i.e. Eq (13). The pre-exponential factor δ_a has the dimension of length and we call it the *adsorption length*. Our definition (14) of δ_a is similar to the one in the theory of adsorption of spherical molecules [59] in the sense that it involves only factors related to the *kinetic energy* of the adsorbed molecules. Eq. (13) is determining also the value of μ_0^S in Eq. (2): $\mu_0^S = \mu_0^B - k_B T \ln K_a = \mu_0^B - E_a - k_B T \ln \delta_a$, cf. also Eq. (3).

S3. Details about the processing of tensiometric data

Here we describe the procedures for processing the experimental tensiometric data and determining the values of the adsorption constants of non-ionic surfactants within the direct approach (Sec. 3.1). Within the direct approach, this is done by fitting the initial region of the experimental surface pressure isotherms with the virial expansion (6) of $\pi^S(C)$.

Let us consider first the adsorption at W|O. Aveyard and Briscoe [32] represented their data for interfacial tension σ of fatty alcohols at W|O as a function of the alcohol concentration C^O in the oil phase. In order to compare these data with results for W|A (where the surfactant is in the water phase), we recalculate the corresponding concentration C in water by using experimental data for the partition coefficient of the alcohols [33] and for the alcohol's tetramerisation constant in the alkane phase [34]. Aveyard and Mitchell [33] studied the partitioning of alcohols (of chain length n from 4 to 7) between water and various alkanes (subscript A; their carbon number n_A vary from 8 to 16). They found that the partition coefficient in dilute solution, $K_p = C^O/C$, depends on the chain lengths both of the surfactant and the alkane. Their data for K_p followed the linear regression model (cf. footnote 5 in the main text):

$$\ln K_p = \ln K_{p0} - n_A \mu_A / k_B T + n\Delta\mu_{CH_2} / k_B T . \quad (46)$$

From numerous independent experimental data, we previously found that $\Delta\mu_{CH_2} = 1.39 \times k_B T$ [8] (see also the S4). By fitting the data of Aveyard and Mitchell [33] with Eq. (46), we determined $\mu_A = 0.057 \times k_B T$ and $\ln K_{p0} = -7.05$. These values differ from those of Aveyard and Mitchell [33] by a few percents since they used three fitting parameters ($\Delta\mu_{CH_2}$ was considered unknown) instead of our two (fixed $\Delta\mu_{CH_2} = 1.39 \times k_B T$).

In order to calculate the surfactant concentration C in water from the experimental values of C^O,

we used the relation $C = \gamma^{O} C^{O}/K_p$. The activity coefficient γ^{O} in the oil phase was calculated by solving the equation $C^{O} = \gamma^{O} C^{O} + 4K_{1,4}(\gamma^{O} C^{O})^4$, where $K_{1,4} = 780$ M^{-3} [34,8] is the tetramerisation constant of the alcohol in the oil phase.

In Sec. 3.1, we used the virial equation (6) to fit the tensiometric data and determine the adsorption constant K_a of the alcohols (in Ref. [8], we used instead the HFL model (1), as in Sec. 3.3). We considered only the experimental data of Aveyard and Briscoe which correspond to $\pi^{S} < 10$ mN/m (the first 5-15 points) – in this region, the effect of the ternary interactions can be disregarded so that Eq. (6) is valid (in contrast to the analysis of the complete adsorption models in Sec. 3.3, where all data points available are taken into account). The fit involves two parameters – the adsorption constant K_a and the second virial coefficient B_2. However, since B_2 is obtained with rather high dispersion, only the values of K_a are of interest and are discussed in the main text. The results are presented in Fig. 3 as $\ln K_a$ vs. n; the regression is illustrated in Fig. 1. The data in Fig. 3 refer to alkane phase varying from octane to hexadecane; unlike the partition coefficient K_p the adsorption constant K_a from water to W|O interface, within the experimental error, seems independent on the length n_A of the alkane molecule. This suggests that the term $-\mu_A n_A$ in Eq. (46) for K_p is related mostly to the state of OH in the oil phase.

Similar fitting procedure with the virial expansion Eq. (6) has been used with the data for *non-cohesive surfactants* at W|A (N-n-alkyl-N,N-dimethylglycine, $C_nH_{2n+1}Me_2N^+CH_2COO^-$, and short chain length homologues of n-alkyl dimethyl phosphine oxides, $C_nH_{2n+1}Me_2PO$) and W|O ($C_{n-1}H_{2n-1}COOH$ with $n = 4$ and 5). The results for K_a so obtained are presented in Fig. 3 and Table 1.

S4. Calculation of the transfer energy $\Delta\mu_{CH_3}$ of the methyl group

In this supplement, we determine the value of the transfer energy $\Delta\mu_{CH_3}$ of a methyl group from oil to water from the data of Abraham for the solubilities in water of alkanes of different chain lengths n_A (*Tables 2 and 3* of Ref. [76]). For the chemical potential of an alkane molecule in the water and alkane phases we use the expressions (cf. *Eq. 19-16* of Hill [59]):

$$\mu^W = \mu_0^W + k_B T \ln \frac{x^W}{v^W}; \quad \mu^O = \mu_0^O + k_B T \ln \frac{1}{v^O}. \tag{47}$$

Here v^W and v^O are molar volumes of water in the water phase and of alkane molecule in the alkane phase respectively; x^W is molar part of the saturated water solution of alkane; $x^W/v^W = C^W$ is the molar concentration of alkane in the water. The standard chemical potentials μ_0^W and μ_0^O involve, first, all internal degrees of freedom of the surfactant molecule, and second, the interaction energy of the molecule with its surroundings (cf. *Eq. 19-5* of Hill [59]). Eqs. (47) lead to the following expression for the equilibrium solubility x^W:

$$\ln x^W = \frac{\mu_0^O - \mu_0^W}{k_B T} + \ln \frac{v^W}{v^O(n_A)}. \tag{48}$$

Assuming that the contributions of the $–CH_2–$ and $–CH_3$ groups are additive (i.e. $\mu_0^W - \mu_0^O = 2\Delta\mu_{CH_3} + (n_A - 2)\,\Delta\mu_{CH_2}$), we can rewrite Eq. (48) as follows:

$$\frac{\Delta\mu_{CH_3}}{k_B T} = -\frac{1}{2}\ln x^W - \frac{n_A - 2}{2}\frac{\Delta\mu_{CH_2}}{k_B T} + \frac{1}{2}\ln \frac{v^W}{v^O(n_A)}. \tag{49}$$

Here $\Delta\mu_{CH_2} = 1.39\times k_B T$ and $v^W = 18.1$ mL/mol; experimental values for x^W and v^O are given in Table S2, together with the values of $\Delta\mu_{CH_3}$ calculated from Eq. (49).

Tanford [77] did not account for the entropic term $\ln(v^W/v^O)$ in Eq (49), which is not negligible – it is of the order of 1-2 $k_B T$ and depends on n_A through the molar volume v^O. Consequently, he obtained different values both for $\Delta\mu_{CH_2}$ and for $\Delta\mu_{CH_3}$ (his 1.49 vs. our $1.39\times k_B T$ and his 3.55 vs. our $2.75\times k_B T$ respectively). The average value for the transfer energy $\Delta\mu_{CH_3}$ for the alkanes in Table S2 is $2.75\times k_B T$, in agreement with the estimate of Ivanov et al. [49].

Table S2. Calculation of the transfer energy $\Delta\mu_{CH_3}$ of a $-CH_3$ from oil to water phase from Eq. (49).

n	[a] $\ln x^W$	[b] v^O [mL/mol]	$\Delta\mu_{CH_3}/k_BT$
5	-11.5	115	2.77
6	-13.1	132	2.8
7	-14.4	147	2.71
8	-16.1	162	2.78
9	-17.7	179	2.85
10	-18.9	194	2.71
12	-21.7	227	2.65
average:			2.75±0.07

[a] Data for solubility x^W of liquid alkanes taken from Abraham [76]; [b] Data for v^O from Refs. [103,104].

S5. The attraction parameter β

In Ref. [16], the expression (22) was used for surfactants with relatively large head groups. For this case, the exponent under the integral can be expanded into series up to the linear term. This leads to an analytical formula for β [16]:

$$\beta = \frac{\pi^{5/2}}{32}\frac{nL_{CH_2}}{l_{CH_2}\alpha^{5/2}k_BT}\arctan\frac{\pi^{1/2}nl_{CH_2}}{2\alpha^{1/2}}. \qquad (50)$$

Even for short chain lengths, Eq. (50) deviates significantly from the exact result (22), cf. Fig. S2. The deviations become larger with the increase of n, especially for surfactants of small actual molecular area α. Therefore, when the model for β is compared with experimental data, we have used the exact result (22) only.

In Fig. S3, the interaction parameter of alcohol films at W|A following from the processing of the experimental data with the SD or the SIAL adsorption models are compared, as functions of the chain length n. The SD model works only if the non-linear dependence (22) is used, while the accuracy of SIAL is acceptable only if combined with the linear Eq. (25).

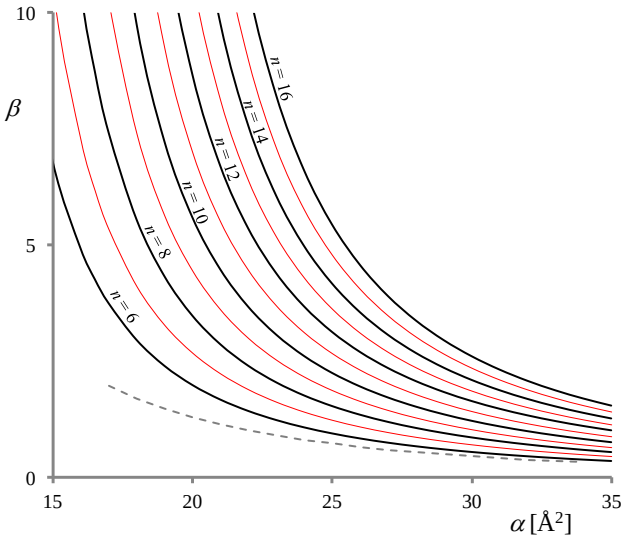

Fig. S2. The attraction parameter β vs. the hard-disc area α of the surfactant, calculated by numerical integration of Eq. (22), at various hydrocarbon chain lengths (from n = 6 to n = 16; black lines are even values of n, red are odd; 25ºC). Dashed line is $\beta(\alpha)$ at n = 6 calculated according to the linearized formula – it is seen that its accuracy is insufficient.

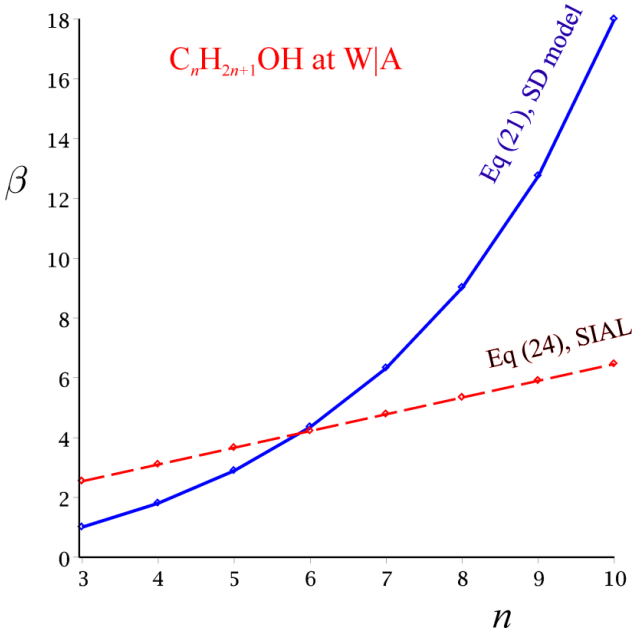

Fig. S3. Attraction parameter β of alcohols (from propanol to decanol) at W|A according to the results from SD and SIAL models. SD model agrees with the tensiometric data for alcohols only in combination with the non-linear model (22) for β. Due to the different approach towards the lateral attraction, SIAL model agrees with the tensiometric data only if the linear dependence is used: $\beta = 0.86 + 0.56n$, see Eq. (25). The combined use of the SD model with Eq. (25), and also of the SIAL model with Eq. (22), strongly disagree with the experiment.

S6. Comparison of various models and fitting procedures against tensiometric data

Table S3 (for alcohols at W|O) and Table S4 (for various amphiphiles at W|A) compare all considered model to tensiometric data for whole homologous series of surfactants. The free parameters of the homologous series are determined via the optimization of merit functions similar to Eq. (29). The most important results are discussed in the main text, Sec. 3.3-3.5; those calculated for completeness and for further reference to the parameter values are discussed briefly here and in S8-S10.

An important from practical viewpoint test is the comparison between all models from Sec. 2.1.2 under the same conditions – 3 free parameters, K_{a0}, α and β. The results are given in rows {8-11} in Table S2. As benchmarks we will use the area α = 16.5 Å^2 following from crystallographic & collapse data, the "direct" value of lnK_{a0} = –21.3 from Table 1, and β = 0.332 obtained with the 2-parametric fit of the SD model, which we consider as reliable. The results lead to the following conclusions: **(i)** the deviations of all 3-parametric models in rows {8-11} are exactly the same. **(ii)** All models yield almost the same value for the adsorption constant K_{a0}, very close to the one directly determined in Sec. 3.1. This is due to the fact that the initial slope of the $\pi^S(C)$ curve (the Henry region) is model-independent. **(iii)** The SD model yields values of α and β closest to the benchmark values. **(iv)** The model of SIAL also gives a value of α close to 16.5 Å^2 but slightly higher β than SD. **(v)** The models of van der Waals and Frumkin give considerably larger values of α (better for vdW), and negative values of β as can be expected from Eqs. (20).

Table S3. Adsorption parameters of $C_nH_{2n+1}OH$ at W|O interfaces, obtained by the minimization of a merit function of the type of Eq. (29).

$C_nH_{2n+1}OH$ at water|alkane[a]	$\ln(K_{a0}/[m])$	α, α_V, α_L [Å^2]	β, β_V, β_L	*dev* [mN/m]
one-parametric fit				
{1} HFL	-20.95	16.5[b]	0	0.49
two-parametric fits				
{2} HFL	-21.1	14.2	0	0.40
{3} Volmer	-21.2	24.4	0	0.39
{4} Langmuir	-21.25	39.0	0	0.40
{5} SD	-21.1	16.5[b]	0.332	0.40
{6} vdW	-21.0	18.2	-1[c]	0.40
{7} Frumkin	-21.0	21.0	-3/2[c]	0.41
three-parametric fits				
{8} SD	-21.1	17.2	0.437	0.39
{9} SIAL	-21.2	15.8	0.556	0.39
{10} vdW	-21.2	24.2	-0.032	0.39
{11} Frumkin	-21.1	35.1	-0.297	0.39

For each model, the assumed fixed values of the parameters are underlined. The transfer energy in the expression (26) for the adsorption constant is fixed to $\Delta\mu_{CH_2} = 1.39\times k_BT$ for all models. The equations defining the adsorption models (first column) are listed in S1. [a] Alcohols are with chain length $n = 8\div18$ (even n only), oil phase is alkane with $n_A = 8\div16$; $T = 20^\circ$C. [b] Value of the area, calculated from data for the crystallographic and collapse area of alcohols. [c] In accordance with Eqs (20), the fixed values $\beta_L = -3/2$ and $\beta_V = -1$ correspond to the lack of attraction ($\beta = 0$).

Table S4. Adsorption parameters of $C_nH_{2n+1}OH$, $C_{n-1}H_{2n-1}COOH$, $C_nH_{2n+1}Me_2PO$ and $C_nH_{2n+1}Me_2N^+CH_2COO^-$ at W|A, obtained by minimization of a merit function of the type of Eq. (29).

model	num. free parameters	range of n[a]	$\ln(K_{a0}/[m])$[b]	α, α_V, α_L [Å^2]	β, β_V, β_L	*dev* [mM/m]
$C_nH_{2n+1}Me_2P^+O^-$ at W|A, n = 7-16, average T = 23.5˚C						
{1} SD	1	7-11/non-coh	-19.9	29[c]	Eq. (22)[d]	1.0
{2} SD	2	7-11/non-coh	-20.0	28.2	Eq. (22)[d]	0.98
{3} SD	2	7-11/non-coh	-21.0	29[c]	0.49(n+1)[e]	1.7
{4} SD	1	7-16/all	-19.7	29[c]	Eq. (22)[d]	2.0
{5} SIAL	1	7-11/non-coh	-20.5	29[c]	0.49(n+1)[e]	1.7
{6} SIAL	3	7-11/non-coh	-20.5	29[c]	-0.08+0.35n	1.0
{7} SIAL	3	7-16/all	-20.6	29[c]	-0.08+0.38n	1.3
{8} vdW	4	7-11/non-coh	-19.9	33.0	-2.46+0.273n	0.91
{9} Frumkin	4	7-11/non-coh	-19.8	43.4	-2.41+0.206n	0.93
$C_nH_{2n+1}Me_2N^+CH_2COO^-$ at W|A, n = 8-16, average T = 20˚C						
{10} SD	2	8-16/non-coh	-21.3	31.0	Eq. (22)[d]	1.8
{11} SD	3	8-16/non-coh	-21.6	30.2	2.31	1.1
{12} SIAL	4	8-16/non-coh	-21.55	23.4	1.93 + 0n	1.1
$C_{n-1}H_{2n-1}COOH$ at W|A, n = 3-10, average T = 21˚C						
{13} SD	1	3-4/non-coh	-20.4	18[c]	Eq. (22)[d]	0.57
{14} SD	1	3-10/all	-20.2	18[c]	Eq. (22)[d]	0.93
{15} SD	2	3-10/all	-20.2	18.2	Eq. (22)[d]	0.92
{16} SIAL	1	3-10/all	-20.4	18[c]	(n +1)0.49[e]	0.94
{17} SIAL	3	3-10/all	-20.7	18[c]	1.44 + 0.46n	0.78
{18} vdW	4	3-10/all	-20.4	22.55	-0.47+0.35n	0.63
{19} Frumkin	4	3-10/all	-20.1	28.8	-1.0 + 0.26n	0.70
$C_nH_{2n+1}OH$ at W|A, n = 3-10, T = 21˚C						
{20} SD	2	3-4/non-coh	-20.1	16.5[c]	Eq. (22)[d]	0.88
{21} SD	1	3-10/all	-20.4	16.5[c]	Eq. (22)[d]	1.44
{22} SD	2	3-10/all	-20.1	17.3	Eq. (22)[d]	1.06
{23} SIAL	1	3-10/all	-20.1	16.5[c]	(n +1)0.49[e]	1.5
{24} SIAL	3	3-10/all	-20.6	16.5[c]	0.86 + 0.56n	0.95
{25} vdW	4	3-10/all	-20.3	20.9	-0.48+ 0.39n	1.1
{26} Frumkin	4	3-10/all	-21.6	31.0	0.97+ 0.26n	1.6

For each model, the assumed fixed values of the parameters are underlined. The equations defining the adsorption models (first column) are listed in S1. [a] Data either only for non-cohesive or for all (cohesive and non-cohesive) homologues are used. [b] For W|A, we use fixed value of the transfer energy $\Delta\mu_{CH_2} = 1.04\times k_BT$. [c] Fixed value of α calculated from the crystallographic and/or collapse areas. [d] Fixed to the value predicted by the nonlinear Eq. (22). Note that the expression (22) for β involves α as a parameter; this was accounted for in the optimization procedure. [e] Fixed value of $\beta_1 = 0.49$ taken from Smith [66].

S7. Analysis of the dispersion of the SD model as a function of the interaction parameters α and β

The two interaction parameters α and β affect the surface pressure isotherm in similar manner and in result they cannot be determined from tensiometric data with good accuracy in most cases. This is valid for all models from Sec. 2.1.2. To illustrate the problem, we will consider the deviation of the SD model, Eqs. (10)-(12), from the data for oil-soluble alcohols (Eq. (29) and row {8} from Table S3). We fixed $\ln(K_{a0}/[\mathrm{m}])$ to its best value, –21.14, and then analysed the merit function $dev(\alpha,\beta)$. This function has a minimum at α = 17.2 Å^2 and β = 0.437; the optimal value of *dev* is 0.392 mN/m. It turns out, however, that the minimum of $dev(\alpha,\beta)$ is rather flat. The deviation is within 1% of the optimal value for any β between 0 and 1 and α between 14 and 21 Å^2, provided that they are related between each other as $\beta = 0.13\alpha - 1.8$ (Fig. S4). This problem is a significant source of errors, especially if data for each homologue is fitted separately. Therefore, fits with both α and β being left as adjustable parameters must be avoided. This means, for example, that the result for β from row {5} in Table S3 (2-parametric SD model with free K_{a0} and β) is far more reliable than the one in row {8} (3-parametric SD model with free K_{a0}, α and β).

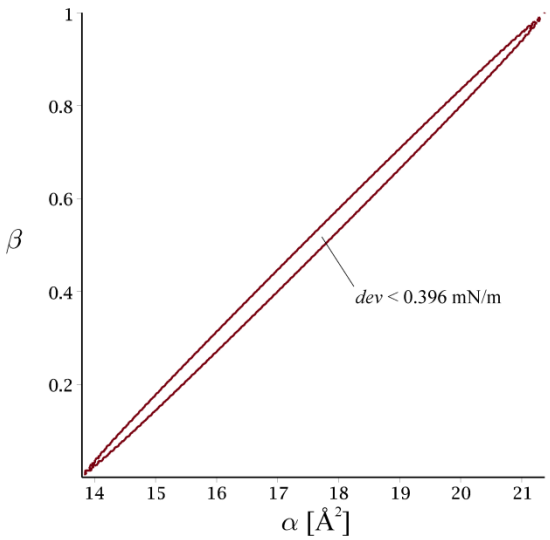

Fig. S4. Standard deviation of the SD model compared to the tensiometric data for oil-soluble alcohols (n = 8÷18) at the W|O interface as a function of α and β. Fixed value $\ln(K_{a0}/[\mathrm{m}]) = -21.14$ is used. It is seen that any value of β between 0 and 1 and any α between 14 and 21 Å^2 can give deviation below 0.396 mN/m (the global minimum is by 1% smaller; any set of adsorption parameters falling inside the ellipse has $dev < 0.396$ mN/m).

S8. Adsorption of the water-soluble non-ionic surfactants at the W|O interface

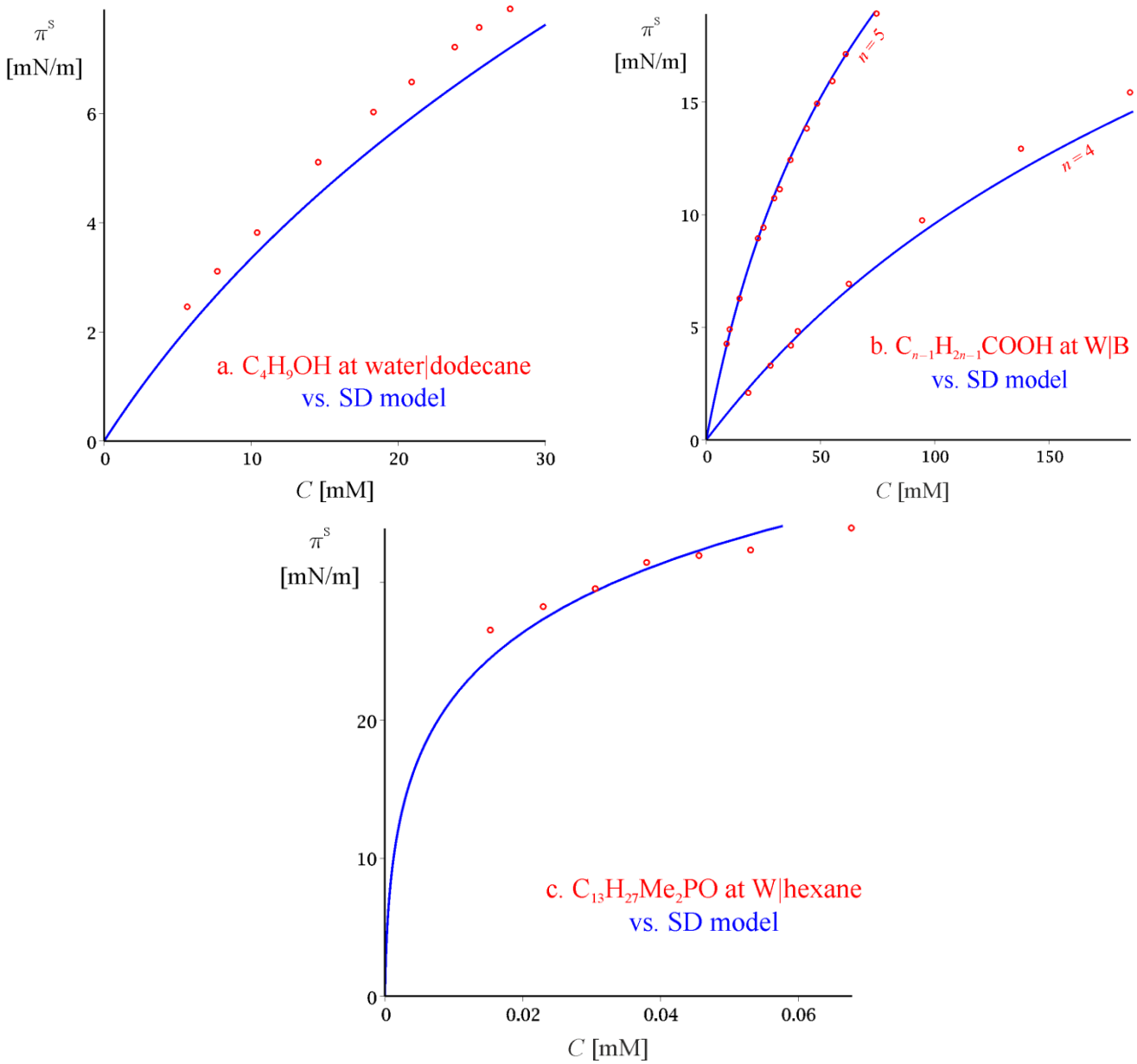

Fig. S5. Interfacial pressure π^S vs. concentration C in the water of several water-soluble surfactants at W|O. **a.** Butanol at water|dodecane, $T = 20^\circ$C. Red points: data from Ref. [82]; blue line: SD model with no fitting parameters (the values of the long-chained oil-soluble alcohols from Table 2 were used). **b.** Butanoic and pentanoic acid at water|benzene, 35ºC. Red points: data from Ref. [72]; blue lines: SD model with $K_{a0} = 2.00$ Å and $\beta = 1.56$. **c.** Tridecyldimethylphosphineoxide at water|hexane, 20ºC. Red points: data from Ref. [83]; blue lines: SD model with $K_{a0} = 1.63$ Å and $\beta \approx 0$.

The findings presented in Sec. 3.3 were about oil-soluble alcohols. In order to verify the obtained results, we analysed also the interfacial tension data for a *water-soluble* alcohol. To the best of our knowledge, only data for butanol, adsorbed at water|dodecane interface are available [82]. We used the SD model with fixed values of the actual area per molecule, α = 16.5 Å^2, and β = 0.332; the adsorption constant is $K_a = K_{a0}\exp(n\Delta\mu_{CH2}/k_BT)$ = 0.169 μm following from the value $\ln(K_{a0}/[m])$ = -21.14 (Table 2). The predicted surface tension isotherm is in good agreement with the experimental data, Fig. S5a. The small positive deviation of the data is probably due to the non-ideality of the aqueous butanol solution, and perhaps the inaccuracy of Eq. (46) for K_p (which can shift the $\ln K_{a0}$ values determined for the oil-soluble surfactants in Table 2 by an additive constant).

The tensiometric data for butanoic and pentanoic acids at the water|benzene (W|B) interface were processed with the 2-parametric SD model (β is assumed independent of n and $\ln K_a$ is assumed to follow Eq. (26) with $\Delta\mu_{CH_2} = 1.39\times k_BT$ as with alcohols at W|O, cf. Sec. 3.3). The result is illustrated in Fig. S5b. Data for a single homologue of the phosphineoxides at W|O is available – it is fitted with the SD model in Fig. S5c. The results are discussed in Sec. 3.3.

S9. Application of the adsorption models to data for N-alkyl-N,N-dimethylglycines at W|A

All homologues of the zwitterionic $C_nH_{2n+1}Me_2N^+CH_2COO^-$ at W|A from Refs. [96,97,86] (n = 8-16) point at weakly cohesive behaviour, suggesting that β is close to 2 (cf. Sec. 3.5). Unfortunately, we found no reliable data for the area per molecule of these surfactants. In addition, the data showed significant disagreement with both Eq. (22) and Eq. (24) for β. This is evident from the high deviation of the SD model with β fixed to the predictions of Eq. (22) (1.8 mN/m, cf. row {10} in Table S4). A 4-parametric fit with SIAL model with assumed linear $\beta(n)$ dependence (Eqs. (8),(9)&(25) with parameters K_{a0}, α, β_0 and β_1) yields β_1 = 0, which means essentially that the attraction parameter β is almost independent of n (row {12} in Table S4). We performed two more tests of this result. The first one was to set $\beta = const$ in the SD model for all $C_nH_{2n+1}Me_2N^+CH_2COO^-$ homologues. This yields a relatively low deviation of 1.1 mN/m and area per molecule close to that of $C_nH_{2n+1}Me_2PO$ (row {11} in Table S4). The second test is following from the fact that if β is not strongly dependant on n, then scaling behaviour similar to the one shown in Fig. 4 for the alcohols at W|O can be expected. Indeed, the SD isotherm (12) can be written as:

$$K_{a0}C\exp\frac{n\Delta\mu_{CH_2}}{k_BT}=\frac{\Gamma}{1-\alpha\Gamma}\left(\frac{2}{1+R_\beta}\right)^{2+1/\beta}\exp\left[\frac{\alpha\Gamma\left(4-3\alpha\Gamma\right)}{\left(1-\alpha\Gamma\right)^2}\times\frac{2}{1+R_\beta}\right], \quad (51)$$

which is similar to Eq. (30). Provided that β is independent of n, Eq. (51) suggests that if π^S is plotted against $C\times\exp(n\Delta\mu_{CH_2}/k_BT)$, where the value $\Delta\mu_{CH_2}/k_BT$ = 1.04 for W|A is used, data for all homologues must fall on a single master curve. This is demonstrated in Fig. S6. Only the most long-chained homologues deviate from the theoretical line predicted by the SD model with constant β.

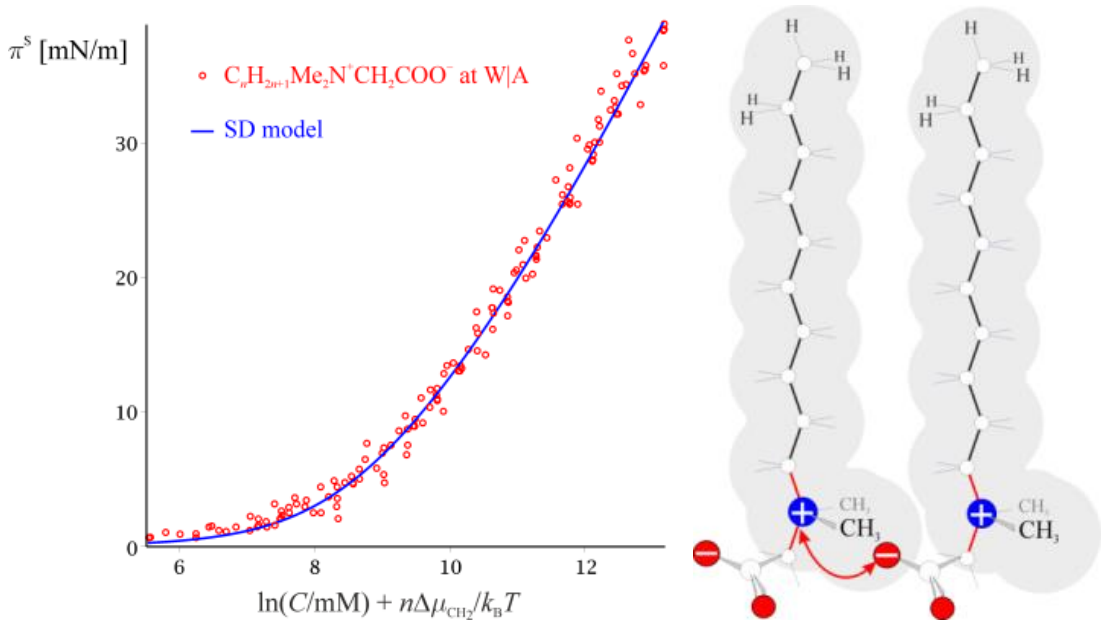

Fig. S6. Surface pressure π^S vs. scaled concentration of N-alkyl-N,N-dimethylglycines at W|A (n = 8-16, T = 20˚C). Data for all homologues fall on a single master curve when plotted in π^S vs. ln[$C\times\exp(n\Delta\mu_{CH_2}/k_BT)$] coordinates (with $\Delta\mu_{CH_2}/k_BT$ = 1.04), in agreement with Eq. (51). The line is calculated via the SD model, Eqs. (10)-(12), with K_{a0} = 4.33 Å, α = 30.2 Å^2 and β = 2.31 (Table 2). The scaling demonstrates that β is independent of n. This fact can be explained with the strong electrostatic attraction between the head groups (illustrated with a red arrow between the positively charged N- and the negatively charged O-atoms in the picture on the right) – seemingly, this interaction dominates over the van der Waals attraction between the hydrocarbon chains.

A possible explanation of the observed little or no dependence of β on n is the following one. Due to the high area per molecule, the attraction between the hydrophobic chains is relatively small, cf. Fig. 2. On the other hand, a very strong electrostatic attraction is possible between the head groups, illustrated in Fig. S6 with a red arrow. If the latter interaction is prevailing (which seems to be true for all homologues with the exception of those with the longest chains), β will indeed depend only on the head group.

The interaction in Fig. 2 is essentially attraction due to the *tangential* component of the large

dipole moment of the $-N^+CH_2COO^-$ head group. The *normal* component of this dipole moment leads to a very long ranged repulsion (which leads to interactions at macroscopic distances [105]!). The contribution of this interaction to the free energy of the surface and the equation of state can be analysed using the approach of Ref. [106], but is complicated by the numerous unknown parameters (surface polarizabilities, bulk quadrupolarizabilities).

S10. Phase transition in the continual approach – the $\pi^S(C)$ isotherm

In this Supplement, the phase behaviour predicted by the SIAL model is considered.

The set of extremum points of Eq. (8) for $\pi^S(\Gamma)$ at any value of β corresponds to the spinodal curve of this EoS, i.e. the spinodal is defined with the condition for extremum, $\partial\pi^S(\Gamma;\beta)/\partial\Gamma = 0$. Substituting here the expression (8) for π^S of the SIAL model and solving, we can find the relation between β and Γ defining the spinodal:

$$\beta_{\text{spinodal}} = \frac{1+\alpha\Gamma}{2\alpha\Gamma\left(1-\alpha\Gamma\right)^3}. \tag{52}$$

Substituting β with β_{spinodal} in the EoS (8), we obtain the spinodal curve in π^S vs. Γ coordinates:

$$\frac{\alpha\pi^{\text{S}}_{\text{spinodal}}}{k_{\text{B}}T} = \frac{\alpha\Gamma\left(1-3\alpha\Gamma\right)}{2\left(1-\alpha\Gamma\right)^3}. \tag{53}$$

The spinodal curve is plotted in Fig. S7a. Below the spinodal curve, no stable phase exists (the mechanical condition for stability, $\partial\pi^S(\Gamma)/\partial\Gamma > 0$, is violated). Between the spinodal and the binodal, only metastable gaseous (on the right of the spinodal) and LE (on the left) phases exist; normally, these metastable phases must pass through a phase transition, forming a heterogeneous film.

To represent the spinodal in π^S vs. C coordinates, we substitute Eq. (52) into SIAL adsorption isotherm (9):

$$\alpha K_{\text{a}} C_{\text{spinodal}} = \frac{\alpha\Gamma}{1-\alpha\Gamma}\exp\left[\frac{-1+2\alpha\Gamma-5\alpha^2\Gamma^2+2\alpha^3\Gamma^3}{\left(1-\alpha\Gamma\right)^3}\right]. \tag{54}$$

Eqs. (53)-(54) define parametrically the spinodal in π^S vs. C (with parameter $\alpha\Gamma$). The result is shown in Fig. S7b-d (red dash-dot line). The cusp of the spinodal corresponds to the coordinates of the critical point.

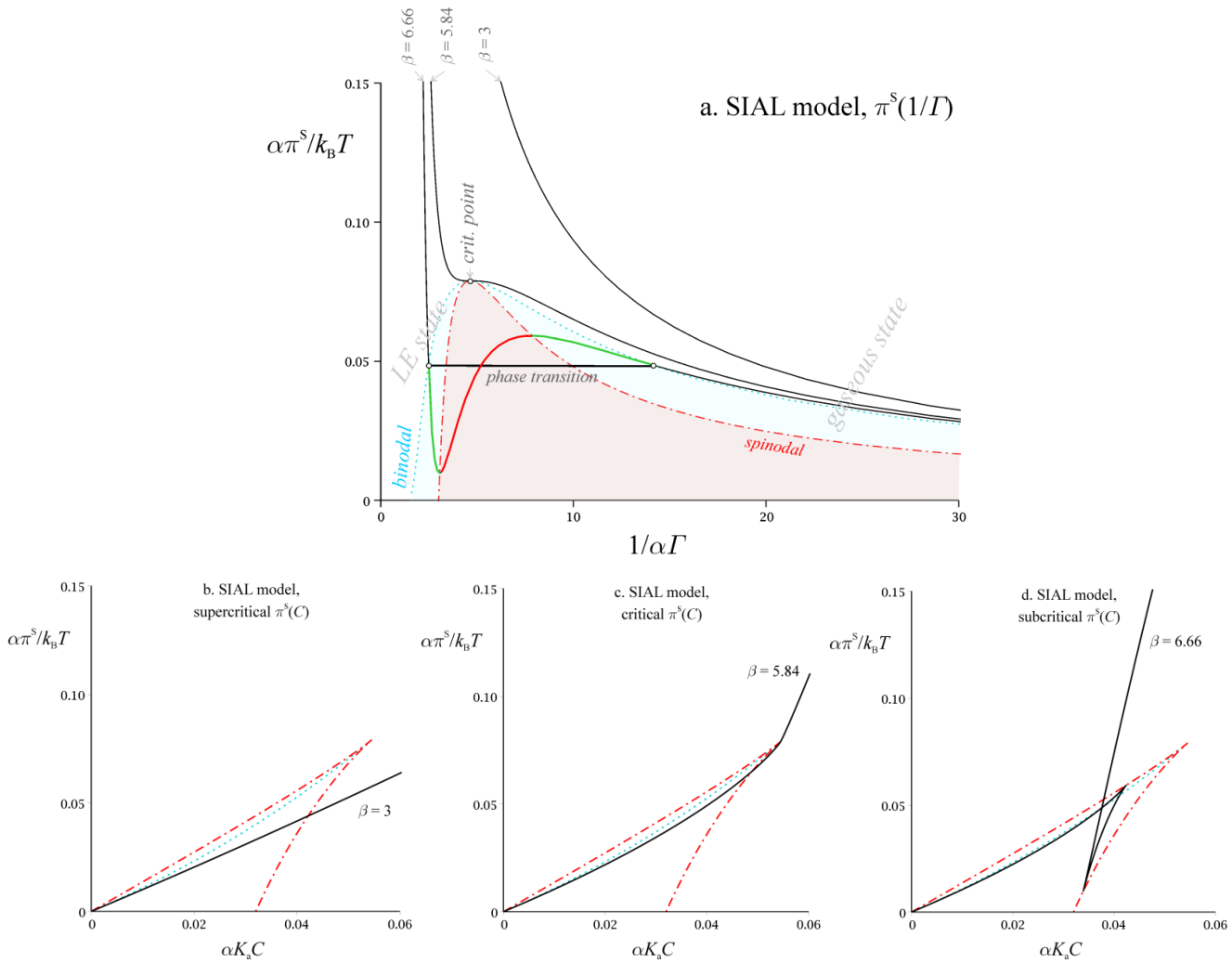

Fig. S7. **a.** Phase diagram in π^S vs. $1/\Gamma$ coordinates (suitably made dimensionless) according to SIAL model, including the spinodal. Below the spinodal stands the truly unstable 2-D fluid. Between the spinodal and the binodal are the metastable gaseous and LE phases. **b-d**. Phase diagram in π^S vs. C coordinates (suitably made dimensionless) for a supercritical, critical and subcritical adsorption layers. Above the critical β, the $\pi^S(C)$ curve has a characteristic intersection point with itself. The intersection point is falling on the binodal and corresponds to the gaseous-LE phase transition. The two cusps falling on the spinodal mark the boundaries of the stable gaseous and LE phase. The branch connecting the two cusps correspond to the unstable state of the layer (corresponding to the part of the $\pi^S(1/\Gamma)$ below the spinodal in **a**).

The SIAL model gives no analytical expression for the binodal curve. The binodal in Fig. S7a is the numerical solution of the conditions for mechanical and chemical equilibrium between the gaseous and the LE phase, $\pi^S(\Gamma^G;\beta) = \pi^S(\Gamma^{LE};\beta)$ and $\gamma^S(\Gamma^G;\beta)\ \Gamma^G = \gamma^S(\Gamma^{LE};\beta)\ \Gamma^{LE}$, where the functions π^S and γ^S are given by Eqs. (8) and by SIAL's surface activity coefficient,

$$\ln \gamma^{S} = -\ln\left(1-\alpha\Gamma\right) + \frac{\alpha\Gamma\left(3-2\alpha\Gamma\right)}{\left(1-\alpha\Gamma\right)^{2}} - 2\beta\alpha\Gamma \ . \qquad (55)$$

compare to Eq. (2). The equilibrium conditions are solved for Γ^{G} and Γ^{LE} for each $\beta > \beta_{cr}$. The obtained Γ^{G} and Γ^{LE} are then substituted in Eqs. (8) and (9) to calculate $\pi^{S}_{binodal}$ and $C_{binodal}$ corresponding to the binodal curve (at the binodal, it follows from the condition for chemical equilibrium that $C^{G} = C^{LE} \equiv C_{binodal}$ and from the mechanical equilibrium that $\pi^{S,G} = \pi^{S,LE} \equiv \pi^{S}_{binodal}$). The result is plotted in Fig. S7a ($\pi^{S}_{binodal}$ vs. $1/\Gamma^{G}$ at $\Gamma < \Gamma_{cr}$ and $\pi^{S}_{binodal}$ vs. $1/\Gamma^{LE}$ at $\Gamma > \Gamma_{cr}$) and Fig. S7b-d (blue dotted line, $\pi^{S}_{binodal}$ vs. $C_{binodal}$). The coexistence curve in π^{S} vs. C coordinates has no two branches and it ends at the critical point.

Additional references

102 S.J. Rehfeld, *J. Phys. Chem.*, 1967, **71**, 738.

103 D.R. Lide (editor), CRC Handbook of Chemistry and Physics, 89th ed. CRC Press/Taylor and Francis, Boca Raton; 2009.

104 R.W. Gallant, C.L. Yaws, Physical properties of hydrocarbons, Vol. 1, 2nd ed. Gulf Publishing Company; 1992.

105 H. McConnell, *Annu. Rev. Phys. Chem.*, 1991, **42**, 171.

106 R.I. Slavchov, I.M. Dimitrova, T. Ivanov, *J. Chem. Phys.*, 2015, **143**, 154707.